Chapter 4

ISOTHERMAL OXIDATION BEHAVIOR OF SUPER AUSTENITIC STAINLESS STEEL 904L AT 500-650 °C

CHAPTER 4

ISOTHERMAL OXIDATION BEHAVIOR OF SUPER AUSTENITIC STAINLESS STEEL 904L AT 500-650 °C

4.1. INTRODUCTION

High temperature oxidation study can be carried out by both cyclic and isothermal exposure of a material. Cyclic oxidation tests are found to be more severe as compared to isothermal test because of alternate stresses generated on the surface due to thermal cycling. However, isothermal oxidation provides an universal as well as independent knowledge of the competing phenomenon occurring during high temperature oxidation [77]. Cao and Norell studied the isothermal oxidation behavior of SASS 904L in humid air atmosphere at 450-600 °C. They showed that the alloy formed a thin oxide layer compared to cyclic oxidation. The damage was less severe for oxidation tests conducted in flowing air conditions [48].

This chapter presents oxidation behavior of the SASS 904L over the temperature range of 500-650 ˚C, in still air, for the duration of 100 h. Apart from the isothermal oxidation behavior in general, a typical feature of formation of pores and pits on the exposed surface is presented in particular. The details of experimental procedures are given in the section 2.3 of Chapter 2.

4.2. RESULTS

4.2.1 WEIGHT GAIN KINETICS

Figure 4.1 shows weight gain/area (ΔW) from exposure at 500-650 ˚C for 25-100 h. During the exposures of 25-50 h, no change was observed in weight from the exposure at

500 ˚C up to 50 h and at 550 °C up to 25 h. There was rapid increase in ΔW at 600 and 650 °C during the initial period of 25 h, thereafter the rate of weight gain was reduced.

To examine the rate law of oxidation kinetics the value of exponent 'n' was determined from the relationship: $\Delta W^n = kt + C$. The value of 'n' varied between 1.5 to 1.8. $\boldsymbol{\Delta W^2 = k_p t + C}$ was used to determine the parabolic rate constants (k_p); where ΔW is weight gain per unit area (mg/cm^2), t is oxidation time in hour and C is a constant. The values of k_p for the respective temperatures are shown in **Figure 4.1b**.

Table 4.1: The phases formed from oxidation at different temperatures during different exposures detected by XRD and Raman spectra.

XRD Analysis					***Raman Spectroscopy***
Temperature (˚C)	**25 h**	**50 h**	**75 h**	**100 h**	**25 h-100 h**
500	γ				Cr_2O_3, Fe_2O_3, Fe_3O_4,
550	γ				Cr_2O_3, Fe_3O_4, $FeCr_2O_4$
600	γ, Cr_2O_3, Fe_2O_3, Fe_3O_4,			γ, Cr_2O_3, Fe_2O_3, Fe_2O_3, NiO	Cr_2O_3, Fe_3O_4, $FeCr_2O_4$
650	γ, Cr_2O_3, Fe_2O_3, Fe_3O_4, NiO				Cr_2O_3, Fe_3O_4, $FeCr_2O_4$

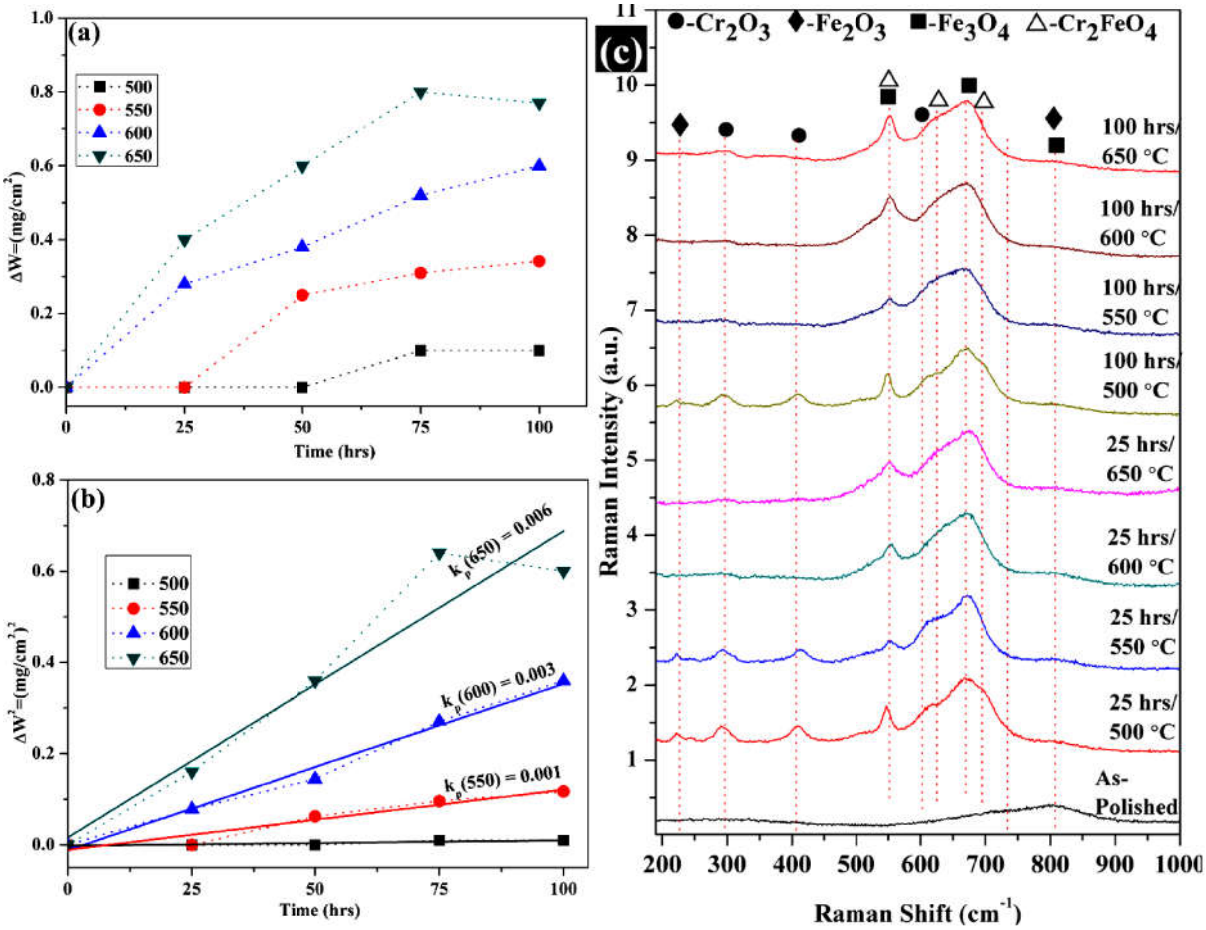

Figure 4.1: Plots of (a) ΔW *vs* t, (b) ΔW^2 *vs* t and (c) Raman spectra of the samples exposed for 25 and 100 h at 500, 550, 600 and 650 ˚C.

4.2.2 PHASE ANALYSIS

Figure 4.2 shows XRD spectra of the samples oxidized at different temperatures. It may be seen that only peaks of γ-Fe are present from the samples exposed at 500 and 550 ˚C. However, there are additional peaks of Cr_2O_3, Fe_3O_4, Fe_2O_3 and NiO from the samples exposed at 500-650 ˚C.

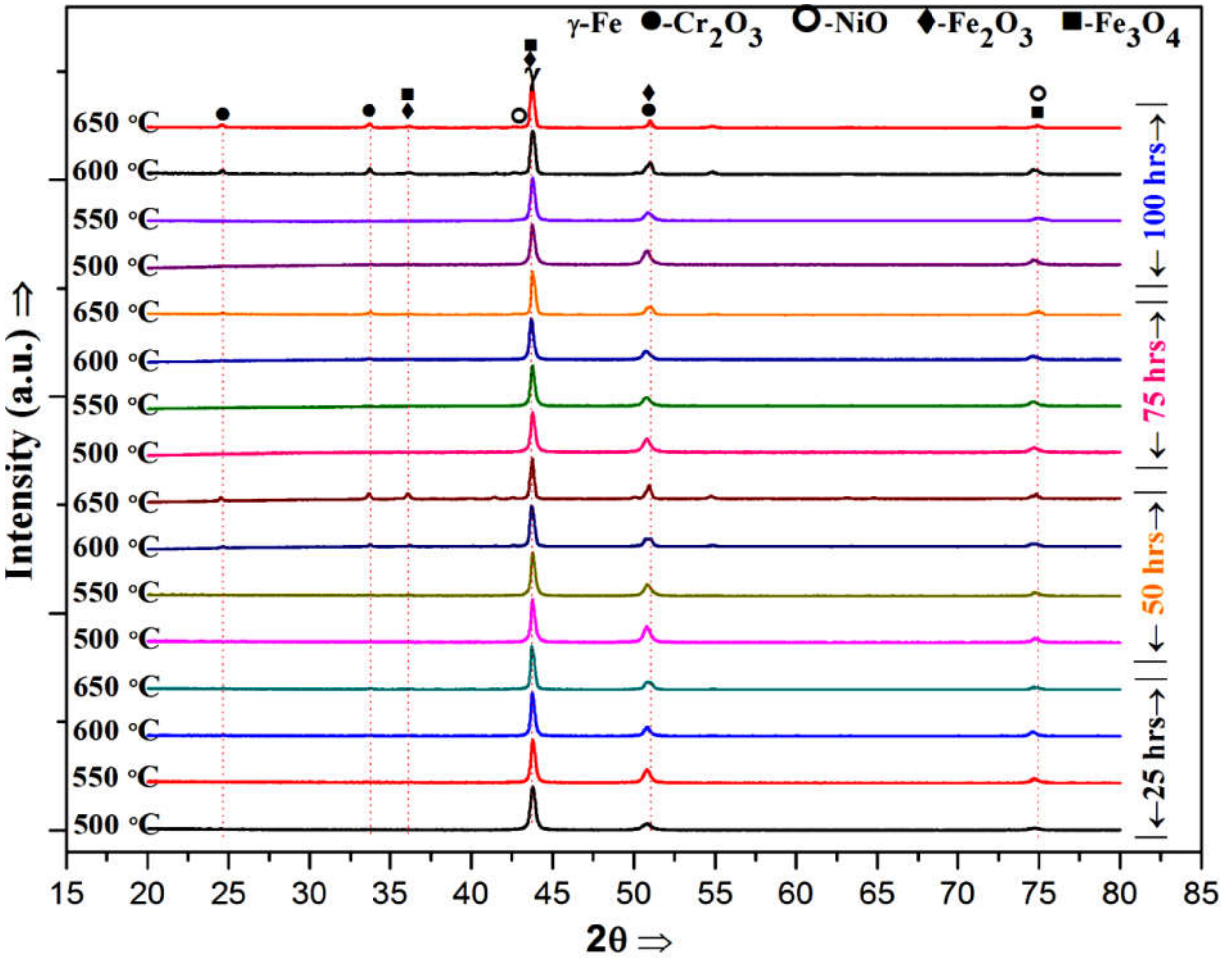

Figure 4.2: XRD spectra of the samples isothermally oxidized for 25, 50, 75 and 100 h at 500-650 ˚C.

4.2.3 RAMAN ANALYSIS

Raman spectra (**Figure 4.1c**) did not show any strong peak of γ for none of the exposed samples and peaks of Cr_2O_3, Fe_2O_3 and $Fe3O_4$ were shown for the sample exposed at 500 °C up to 100 h. The peaks of different oxides and spinels of oxides for the samples exposed at different temperatures and durations are shown in **Table 4.**

4.2.4 SEM ANALYSIS

Figures 4.3(A-I) and (a-i) show SE and BSE mode images respectively. **Figure 4.3(A,a)** shows these images of the as-polished sample and **Figure 4.3(B-i)** presents the image of surfaces of the samples oxidized at 500-650 ºC for 25 and 100 h. SE images clearly show oxide nodules, whereas BSE images show distinct pores, on all the exposed samples. The number density of pores was highest on the sample exposed at 500 °C for 25 h (**Figure 4.3b**). It was slightly less for the sample exposed for 100h; however, the size was relatively larger (**Figure 4.3c**). The pores were seen relatively more on the crest of the mechanically polished surface. The number density of pores decreased with increase in temperature due to faster kinetics of oxide formation and filling of some pores by oxides and the size of the remaining pores increased with temperature and duration of exposure. Clustering and coalescence of pores, led to formation of pits (**Figure 4.3(h,i)**). EDX analysis of the oxide clusters and pits showed difference in relative concentration of the different alloying elements (**Figure 4.4**).

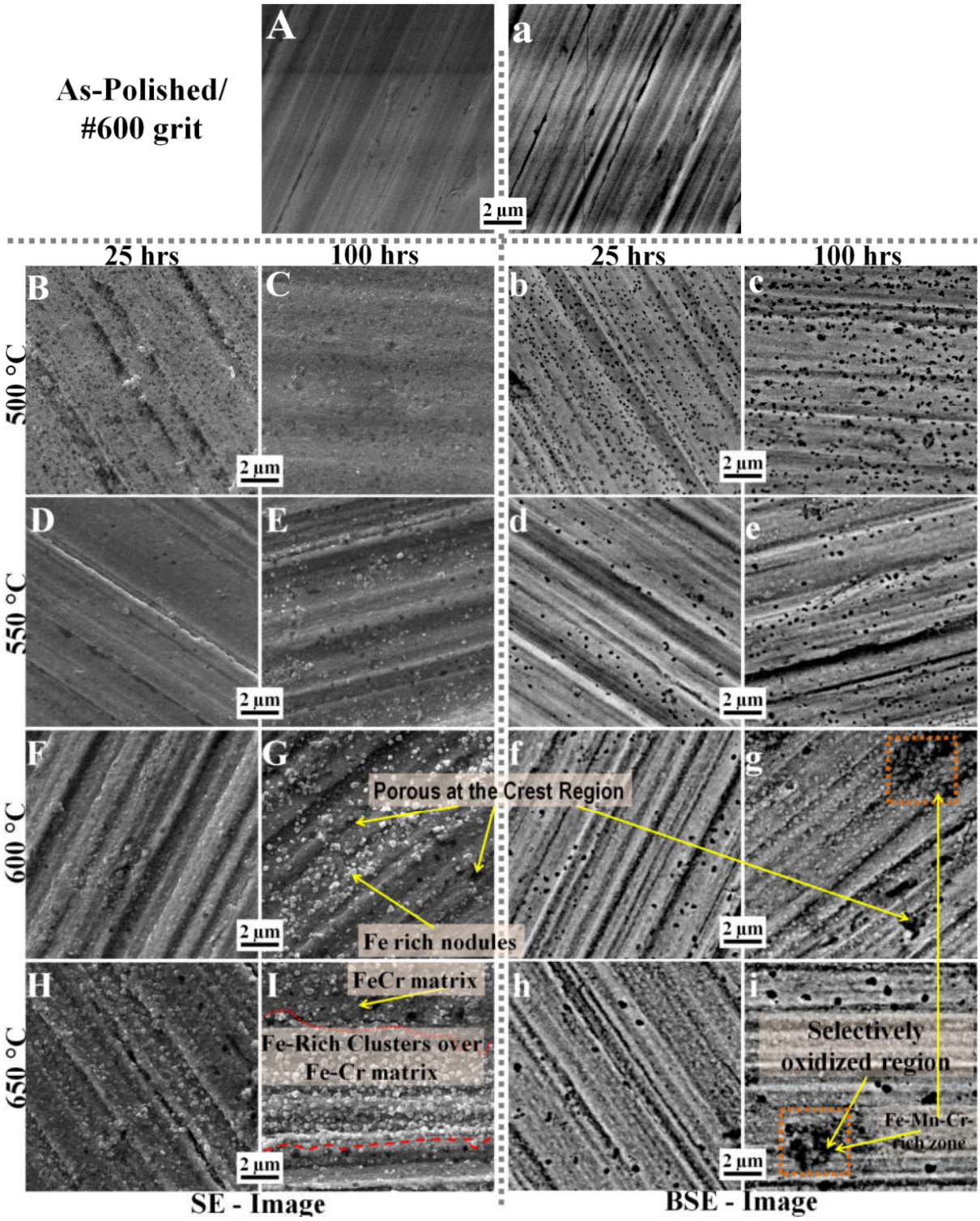

Figure 4.3: SE and BSE images showing surface morphology of: (A,a)as-polished (unexposed) sample and the samples exposed isothermally for 25 and 100 h at: (B,C,b,c)500; (D,E,d,e)550; (F,G,f,g)600; and (H,I,h,i)650 °C, respectively in air atmosphere.

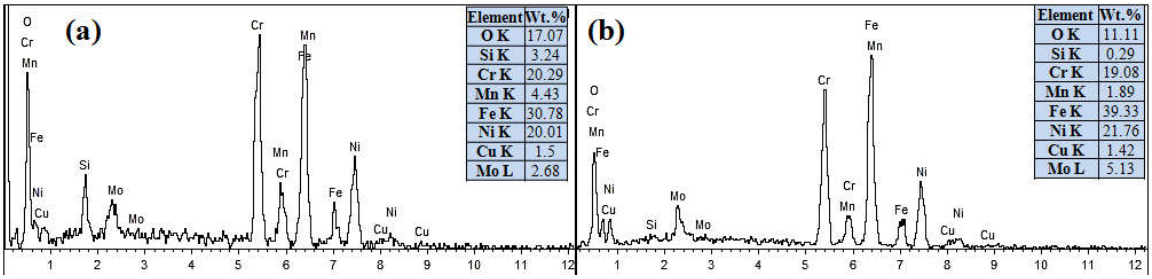

Figure 4.4: EDX analysis of the oxidized surface from: (a) clusters of pores and (b) clusters of oxides.

4.2.5 EPMA ANALYSIS

Figures 4.5 to 4.8 show EPMA analysis of cross sections of the samples isothermally oxidized at 650 ˚C for 25, 50, 75 and 100 h. The images of cross sections are in BSE mode and the colored images are relatively sharp. **Figure 4.5** shows image of cross section and mapping of O, Cr, Fe, Mo, Mn and Ni. There is formation of very thin oxide layer, the enrichment of oxygen is quite evident. However, there is discontinuous distribution of oxygen and variation in its concentration. There is slight decrement in concentration of Cr at the surface, whereas there is no observable change in concentration profiles of the other elements. **Figure 4.6** shows features of cross section of the samples oxidized for 50 h, which appears to be similar to that oxidized for 25 h (**Figure 4.5**). However, the concentration of oxygen is relatively more in **Figure 4.6**. There is discontinuity and variation in the concentration of oxygen on the oxidized surface. There is slight enrichment of Fe, Mo and Ni in the oxide layer. **Figure 4.7** shows behavior of the sample exposed for 75 h at 650 ˚C. The distribution of oxygen in this sample also is similar to those observed in **Figures 4.5 and 4.6**. While there is decrement in concentration of Cr in the region close to substrate there is localized enrichment in some regions as seen on the left side. There is

depletion of Fe on the top surface. There is slight enrichment of Mo on the top surface. There are observable differences in concentration profiles of the different elements in surface region of cross section of the sample oxidized for 100 h (**Figure 4.8**). There is much enrichment of oxygen in the central region and on the right side. The concentration of oxygen is much less on the left side. Thus, there is much variation in oxygen content of the oxide layer from one to other region. While, there is depletion of Cr in most of the region at the top surface, there is also localized enrichment of oxygen as seen on the right side. There is non-uniform enrichment of oxygen above the substrate. There is depletion of Ni at the uppermost surface, varying from one region to other. There is slight enrichment of Ni above the substrate.

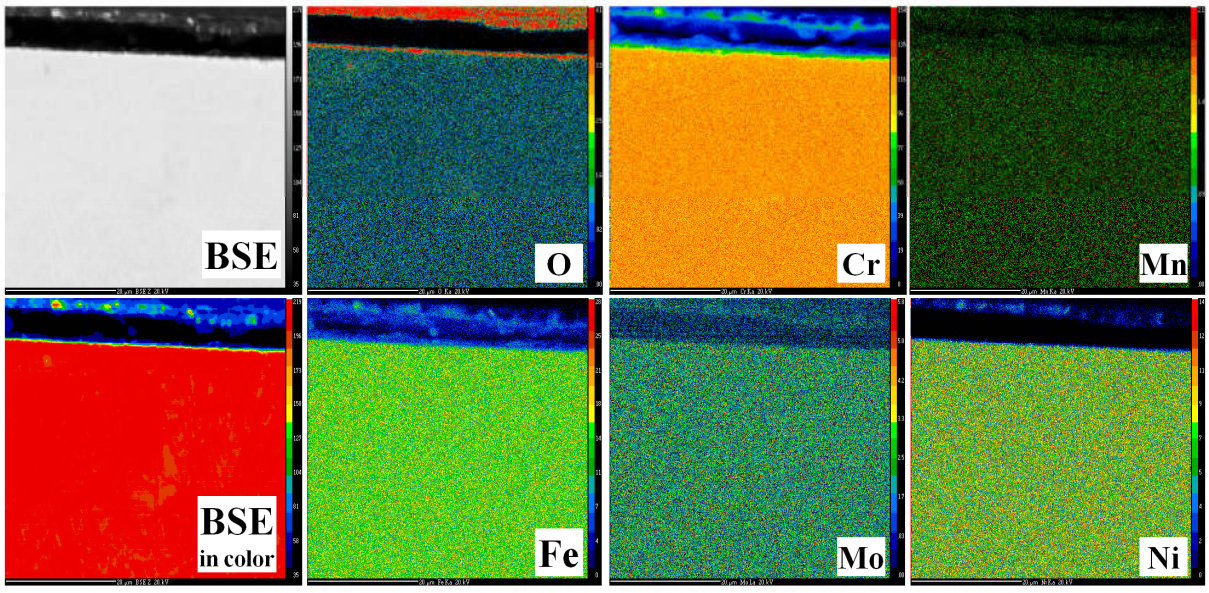

Figure 4.5: EPMA analysis of the cross section of the sample exposed for 25 h at 650 ˚C.

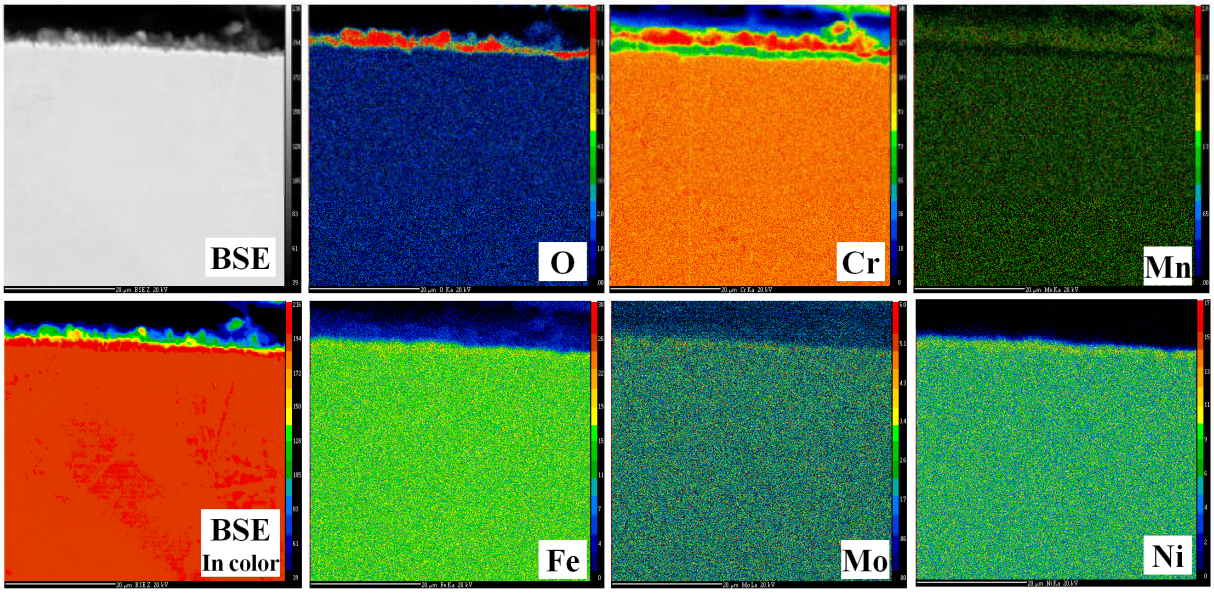

Figure 4.6: EPMA analysis of the cross section of the sample exposed for 50 h at 650 ˚C.

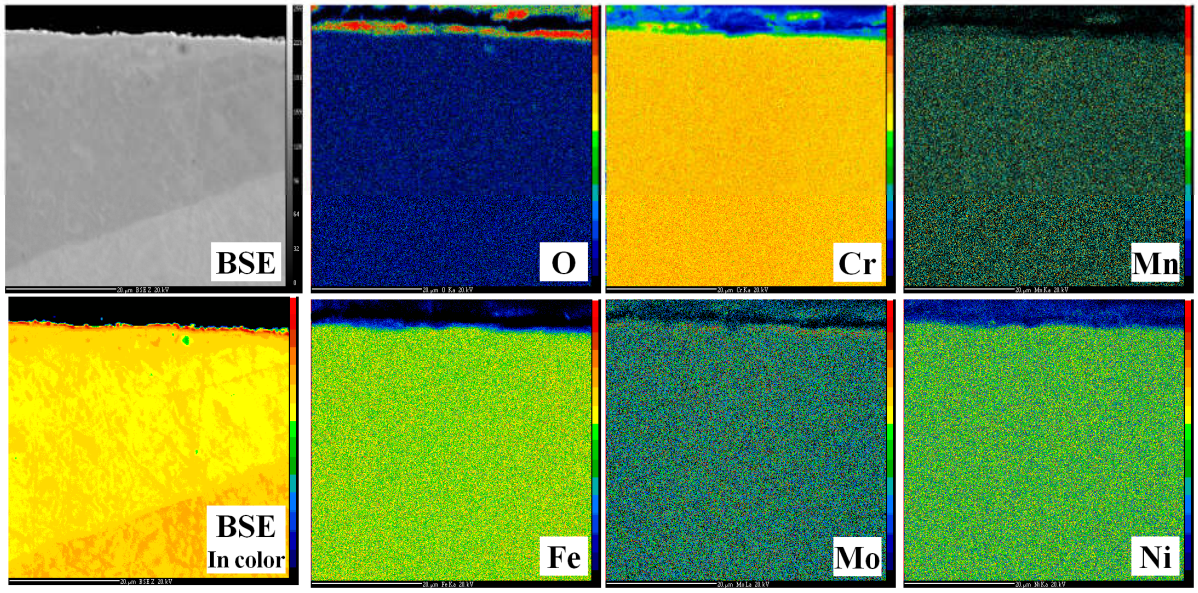

Figure 4.7: EPMA analysis of the cross section of the sample exposed for 75 h at 650 ˚C.

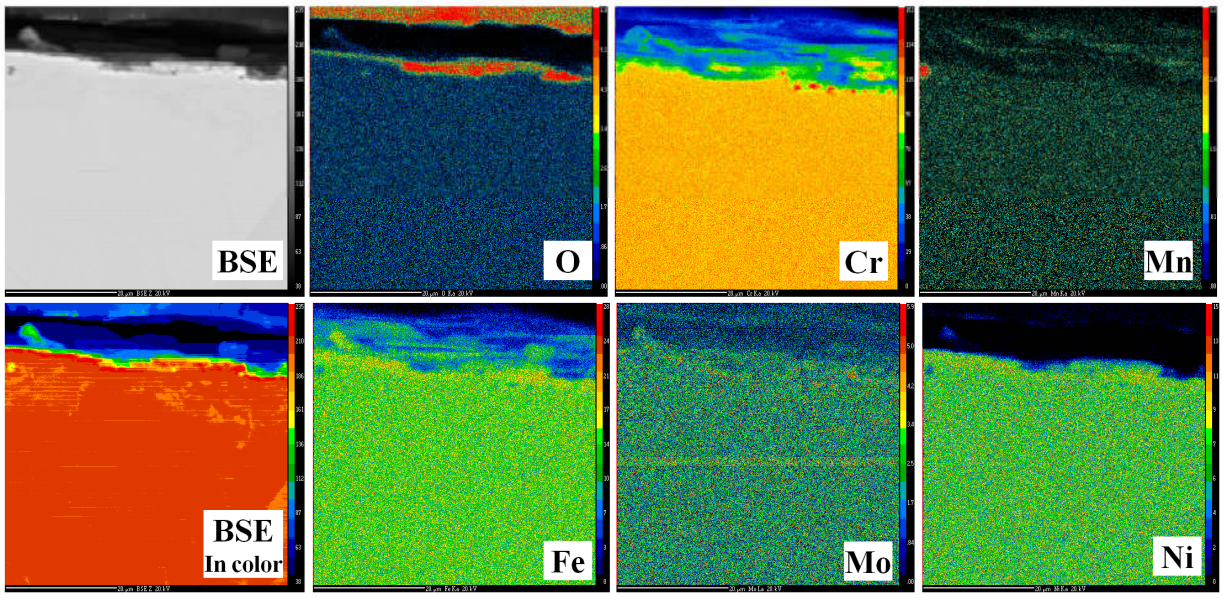

Figure 4.8: EPMA analysis of the cross section of the sample exposed for 100 h at 650 ˚C.

4.3. DISCUSSION

As mentioned in section 4.2, the data of weight gain per unit area (ΔW) was analysed as per the equation $(\Delta W)^n = kt$, where k is rate constant and t in hours is the time period of exposure. As mentioned in the section 4.2.1 '*n*' value was found to lie in the range of 1.5-1.8. Thus, it is obvious that near parabolic rate law of oxidation was exhibited during the isothermal exposure in air in the temperature range from 500-650 ˚C.

It is evident from **Figure 4.1(a,b)**, showing the plot of ΔW *vs* t and ΔW^2 *vs* t respectively, that there was marked influence of the temperature of exposure on the rate of oxidation. While from 500 ˚C of exposure, the plot of $(\Delta W)^2$ *vs* t does not show any observable slope, there is progressive increase in the slopes with rise in temperature from 550-650 ˚C, likewise the kp value increases from 0.01-0.06 respectively. The values of kp corresponding to different temperatures of exposures from 550-650 ˚C are shown along

with the plots corresponding to different temperatures of exposures (**Figure 4.1b**). It may be seen from **Figure 4.1b** that at 600 and 650 ˚C, there was rapid increase in ΔW up to 25 h of initial exposure.

However, the slope of the plots continuously decreased with the duration of exposure up to the exposure of 100 h, carried out in the present investigation. A similar behavior may be seen also at the lower temperatures of exposure, at 500 and 550 ˚C from the exposure of 50-100 h. This behavior may be understood due to formation of protective oxide layer on the surface.

Such type of oxidation behavior has been reported in highly alloyed stainless steels such as Fe-Ni-Cr [78], as well Fe-Cr [79]. **Table 4.1** shows that based on XRD analysis, there is presence of only austenite (γ) phase in the specimens oxidized at 500 and 550 ˚C whereas Raman spectroscopy shows presence of Cr_2O_3, Fe_2O_3 and Fe_3O_4 oxides on the specimens exposed even at these lower temperatures. On the other hand, from the higher temperature of exposure (600 and 650 ˚C), oxide phases are revealed also by the XRD, because of their higher volume fraction (≥5%). The presence of austenite (γ) in all the specimens exposed from 500-650 ˚C is due to much higher depth of penetration of the X-rays. However, from this observation it is obvious that all the phases resulting from the oxidation from 500-650 ˚C were exposed to X-rays, though some of them with low volume fraction could not be analysed by XRD. On the other hand, Raman spectroscopy did not show the γ phase even in the samples oxidized at the lowest temperature of 500 ˚C but revealed the presence of the oxide phases. Thus, it is essential to utilize such sensitive analysing tool for characterization of the phases resulting from exposures at elevated temperatures, formed even in much less amount and in very thin layer on the surface.

In most of the investigations related to oxidation of ferrous structural material, much attention has been paid on formation and characterization of the different oxides and spinels of oxides and no attention has been paid to formation of voids on the surface. These features could be observed in the BSE mode image. As shown in **Figure 4.3** formation of large pit/void types of features could adversely affect the integrity of the structural component, particularly under cyclic loading, due to increased stress concentration and easy crack initiation. It may be seen from **Figure 4.4** that there is considerable variation in concentration of the different elements in the clusters of oxide nodules and the clusters of pores. Thus, it is evident that there could be considerable difference in oxidation kinetics of the material in localized regions of pores and nodules.

It is evident from the EPMA analysis that there is much variation in the nature of the oxide layer formed at different temperatures of exposure in terms of the distribution and concentration of oxygen and the other elements from one to other region. Formation of a discontinuous protective oxide is unlikely to enhance oxidation resistance at elevated temperatures. It is seen that different types of oxides and spinels of oxides form under different conditions of exposure.

4.4. CONCLUSION

1. Isothermal exposure of SASS 904L at 500-650 ˚C in air for the durations up to 100 h exhibits near parabolic rate law. The value of the parabolic rate constant (kp) increases progressively from 500-650 ˚C of exposure.

2. The weight gain per unit area (ΔW) increases rapidly during the initial period of exposure, up to 25 h, and the rate of weight gain progressively decreases with the duration of exposure.

3. Characterization of the isothermally oxidized samples at 650 ˚C in BSE mode revealed unique clusters of pits. The size of such pits/voids on the oxidized surface increased with the duration of exposure, though the number density was found to decrease. Coalescence of such pits/voids led to formation of larger size surface defects, which could be detrimental particularly under cyclic loading.

4. Formation of different oxides such as Cr_2O_3, Fe_3O_4 and spinels of oxides ($FeCr_2O_4$) was observed, depending on the temperature of exposure.

5. EPMA analysis of the oxidized samples showed variation in concentration and distribution of oxygen and other elements on the surface of the samples oxidized at 500-650 ˚C up to 100 h.